

## **DISCLAIMER**

**This report was prepared as an account of work sponsored by an agency of the United States Government. Neither the United States Government nor any agency thereof, nor any of their employees, makes any warranty, express or implied, or assumes any legal liability or responsibility for the accuracy, completeness, or usefulness of any information, apparatus, product, or process disclosed, or represents that its use would not infringe privately owned rights. Reference herein to any specific commercial product, process, or service by trade name, trademark, manufacturer, or otherwise does not necessarily constitute or imply its endorsement, recommendation, or favoring by the United States Government or any agency thereof. The views and opinions of authors expressed herein do not necessarily state or reflect those of the United States Government or any agency thereof. Reference herein to any social initiative (including but not limited to Diversity, Equity, and Inclusion (DEI); Community Benefits Plans (CBP); Justice 40; etc.) is made by the Author independent of any current requirement by the United States Government and does not constitute or imply endorsement, recommendation, or support by the United States Government or any agency thereof.**

**LA-UR-25-25325**

**Approved for public release; distribution is unlimited.**

**Title:** DARHT Axis 1 Bremsstrahlung Dose Measurements

**Author(s):** Moir, David C.; Jaworski, Michael Andrew; Abdallah, Kimberly Lynn; Brooks, Robert Lee; Gonzales, Andrew Geronimo; Ortiz, Gabriel Thomas; Ronquillo, Daniel; Sanchez, Manolito; Snider, Samuel Eugene II

**Intended for:** Report

**Issued:** 2025-10-21 (rev.1)



Los Alamos National Laboratory, an affirmative action/equal opportunity employer, is operated by Triad National Security, LLC for the National Nuclear Security Administration of U.S. Department of Energy under contract 89233218CNA00001. By approving this article, the publisher recognizes that the U.S. Government retains nonexclusive, royalty-free license to publish or reproduce the published form of this contribution, or to allow others to do so, for U.S. Government purposes. Los Alamos National Laboratory requests that the publisher identify this article as work performed under the auspices of the U.S. Department of Energy. Los Alamos National Laboratory strongly supports academic freedom and a researcher's right to publish; as an institution, however, the Laboratory does not endorse the viewpoint of a publication or guarantee its technical correctness.

**UNC**

# DARHT Axis 1 Bremsstrahlung Dose Measurements

Ocotillo

D C Moir, M A Jaworski, K Abdallah, R Brooks, G Gonzales, G  
Ortiz, D Ronquillo, M Sanchez, O Sneddon, S Snider

LA-UR-25-25325  
June 18, 2025

**Contents**

<b>1</b>	<b>Introduction</b>	<b>1-1</b>
<b>2</b>	<b>Experiment Layout</b>	<b>2-1</b>
<b>3</b>	<b>Calorimeter</b>	<b>3-1</b>
<b>4</b>	<b>Diamond Radiation Detector (DRD)</b>	<b>4-1</b>
<b>5</b>	<b>Compton Diode (CD)</b>	<b>5-1</b>
<b>6</b>	<b>Simple Scaling and xtr with Dosecalcx Calculations</b>	<b>6-1</b>
6.1	Scaling	6-1
6.2	Dosecalcx and xtr	6-2
<b>7</b>	<b>Conclusion</b>	<b>7-1</b>
	<b>References</b>	<b>R-1</b>

**Figures**

2-2	70mm and 55mm xtr beam transport through the Axis 1 accelerator	2-2
3-1	Plot of the resistance change across the Resistance Temperature Detector as a function of time in seconds	3-1
4-1	Photographs of the Diamond Radiation Detector (DRD) used on DARHT Axis 1	4-1
4-2	Circuit diagram of diamond diode on DARHT Axis 1	4-1
4-3	Digitized waveforms from the Diamond Radiation Detector (DRD) for both 55mm (Shot number: 39253) and 70mm (Shot number: 39290) cathodes — a) is raw waveform with 50V bias, and b) is the integrated waveform	4-2
5-1	Drawing of a slice through the center of the Compton diode	5-1
5-2	Circuit diagram of Compton diode on DARHT Axis 1	5-1
5-3	Digitized waveforms from the Compton diode for both 55mm (Shot number: 39253) and 70mm (Shot number: 39290) cathodes — a) is raw waveform, and b) is integrated waveform	5-2
6-1	Digitized waveforms from the BPM 25 (black) and 26 (red) for both a 70mm cathode (Shot number: 39290) and a 55mm cathode (Shot number: 39256)	6-2
6-2	Twiss plots calculated by xtr for transport from BPM26 to the target for 55mm and 70mm cathode using respective xtr tunes.	6-3
6-3	DRD (a) and CD (b) for 55mm (Red) and 70mm (black) with Dosecalcx scaled values for 55mm waveforms	6-3

**Tables**

2-1	Layout of the Ocotillo experiment on DARHT Axis 1	2-1
3-1	Summary of the calorimeter results for the 55mm and 70mm cathodes	3-1

# **UNC**

## **Contents**

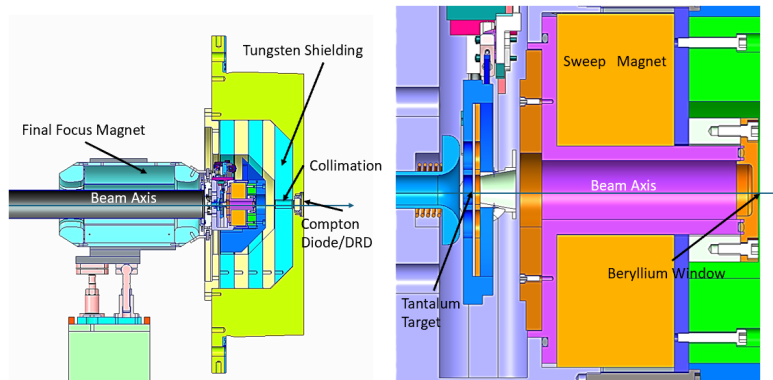
6-1	Summary of the accelerator parameters for the 55mm and 70mm cathodes . . . . .	6-1
6-2	Summary of the Dosecalcx input parameters for the 55mm and 70mm cathodes . . . . .	6-2
7-1	Ratios of radiation measurements for 55mm and 70mm cathodes . . . . . . . . . . .	7-1

## **1 Introduction**

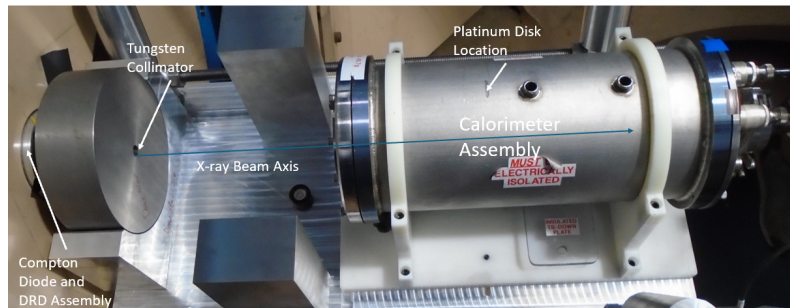
The Dual-Axis Radiographic Hydrodynamic Test (DARHT) facility provides flash radiography capabilities using two electron Linear Induction Accelerators (LIA's). Axis-1 of DARHT produces, nominally, a 20-MeV, 1.5-kA, 80-ns-Full Width at Half Max (FWHM) electron beam. The electron beam is focused on to a tantalum target to produce a Bremsstrahlung x-ray dose for flash radiography of dynamic systems. This paper will describe and compare a variety of techniques for determining the x-ray dose for two different beam currents produced by a 55mm and 70mm diameter cathode. The data was taken in November of 2022 on DARHT Axis 1. The experimental measurement techniques include a platinum calorimeter, a diamond radiation detector (DRD), and a Compton diode (CD). Gafchromic EBT3 self-developing dosimetry film was also used, but no useful results were obtained. Beam charge and energy were recorded and dose was calculated with this information using xtr with Dosecalcx, and simple dose charge-energy scaling. In this paper, we will discuss the target geometry and experimental layout, the methods of measuring dose, dose diagnostics and measurement of beam charge and energy, and the comparisons of data and calculations.

## 2 Experiment Layout

Our experimental setup, carefully designed to compare dosimetry measurement techniques, can be seen in the following Figures, 2-1a and 2-1b. Figure 2-1a provides a comprehensive overview of the Axis 1 Final Focus Magnet, including details of the target assembly, and Figure 2-1b is a photograph of the Ocotillo experiment set-up.



(a) Schematic of DARHT Axis 1 final focus and target regions



(b) Layout of the Ocotillo experiment

Furthermore, Table 2-1 provided below presents a more detailed breakdown of the spacing and arrangement of the various elements involved in the experiment, which are clearly shown and labeled in both Figures 2-1a and 2-1b.

Element	Location (mm)	Radius (mm)	Angle from Source (degrees)
Target	0.0	0.010	0
Be Window	124	12.5	5.78
Shielding Collimation	167	12.5	4.28
Compton Diode	267	35.0	7.51
Diamond Radiation Detector	272	0.5	0.10
Collimator Face	289	5.0	0.99
Collimator Downstream	340	5.0	0.84
Calorimeter Entrance Window	529	25.0	2.71
Platinum	633	15.4	1.4

Table 2-1: Layout of the Ocotillo experiment on DARHT Axis 1

## Experiment Layout

The accelerator beam charge and energy for the 70mm and 55mm cathodes at the target are  $19.30 \pm 0.02$  and  $19.6 \pm 0.03$  MeV, and  $0.170 \pm 0.001$  and  $0.111 \pm 0.001$  mC, respectively, and a pulse width of 80ns-FWHM. In figure 2-2, the predicted accelerator beam envelopes for the 70mm and 55mm cathodes calculated using xtr can be seen [1].

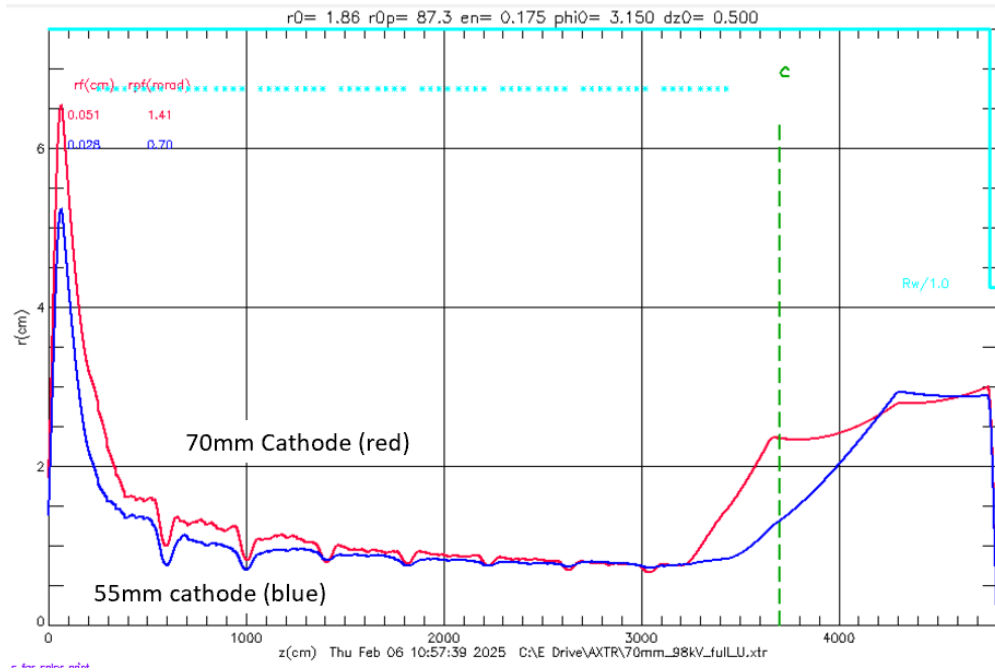


Figure 2-2: 70mm and 55mm xtr beam transport through the Axis 1 accelerator

In the experiment, the limiting aperture for the uncollimated experiments acted as the shielding collimation, where the opening half-angle relative to the beam axis was  $4.28^\circ$ . This angle corresponds to a radiation distribution diameter of 52.9 mm at the location of the platinum disc within the calorimeter. With the collimator installed, the beam size at the point of the platinum was measured to be 10.1 mm in diameter, notably smaller than the diameter of the platinum disc itself with a diameter of 15.4 mm. Due to this difference, proper and careful alignment of the calorimeter is critical, but it is worth noting that no effort was made to verify or ensure the alignment during the experiment, potentially impacting the accuracy of the results. Now let us look over the calorimetry method.

### 3 Calorimeter

Calorimetry was the first tested method for direct measurement of the radiation dose. The technique is described in detail by Watson, et. al. in [6]. Equation 11 from [6] is given as:

$$Dose = 7.3 \cdot 10^3 \left( \frac{\Delta R}{d^2} \right) \quad (1)$$

for  $d > 1\text{m}$ , where  $\Delta R$  is the change in resistance measured by a bridge.

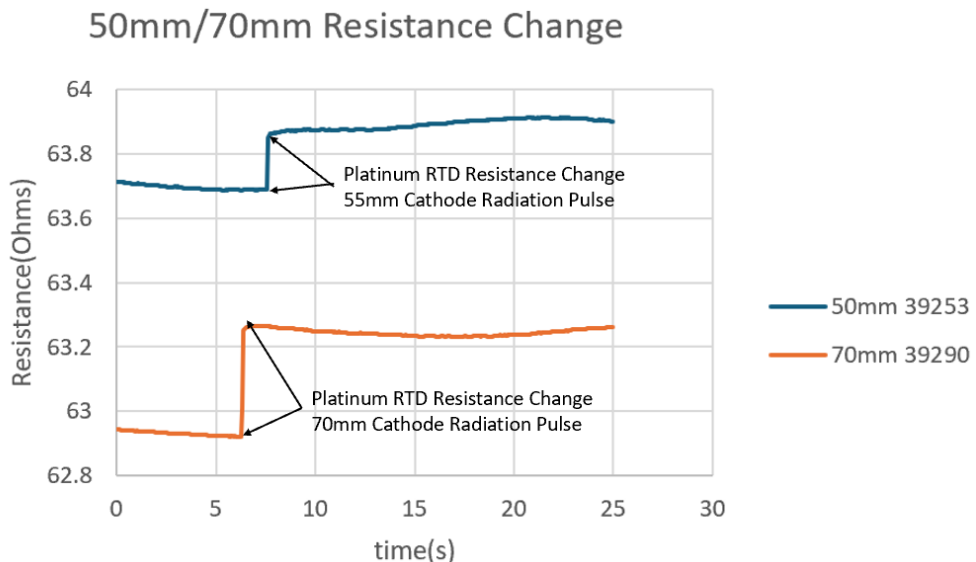


Figure 3-1: Plot of the resistance change across the Resistance Temperature Detector (RTD) bridge measurement for the 55mm and 70mm cathode radiation pulses.

Figure 3-1 is a sample of the  $300\Omega$  Platinum Resistance Temperature Detector (RTD) bridge measurement for the 55mm and 70mm cathode radiation pulses.

FF Magnet (A)	Cathode Size/samples	Collimator Dose (R)	No Collimator Dose (R)	Ratio
396	55mm/5	$175 \pm 4$	$457 \pm 6$	$2.61 \pm 0.03$
403	70mm/5	$376 \pm 18$	$839 \pm 16$	$2.23 \pm 0.05$

Table 3-1: Summary of the calorimeter results for the 55mm and 70mm cathodes

Table 3-1 summarizes all of the calorimeter results for Ocotillo on Axis 1, including the Final Focus Magnet settings, the cathode size and number of beam shots taken, the measured doses at 1m from the target with the 10mm diameter collimator both installed and uninstalled, and finally, the ratio of dose without and with the collimator. Given the nature of "on-axis dose", it was expected that these ratios would be close to one. The ratio values are clearly not. Finally, the ratio is given as:

$$\frac{D_{70mm}}{D_{55mm}} = 1.84 \pm 0.02 \quad (2)$$

## 4 Diamond Radiation Detector (DRD)

The next method of radiation dosage measurement we will discuss involves the use of a Diamond Radiation Detector, or a DRD. The radiation hardness of diamond and its high saturation velocity make it an ideal material for use in radiation detection.

The detector consists of a 1 x 1 x 1 mm diamond crystal mounted on the tip of ridged coaxial cable, where one side of the crystal is attached to the cable center conductor and the other side to the ground of the cable, as seen in Figure 4-1.

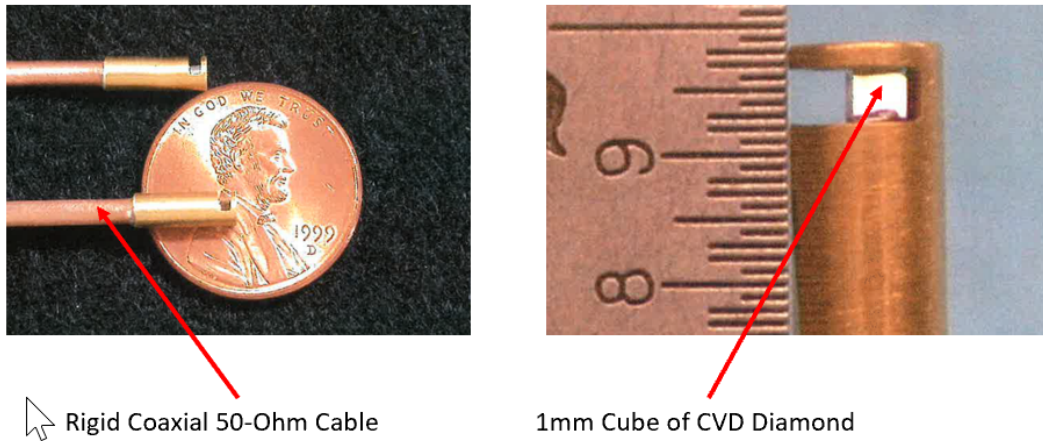


Figure 4-1: Photographs of the Diamond Radiation Detector (DRD) used on DARHT Axis 1

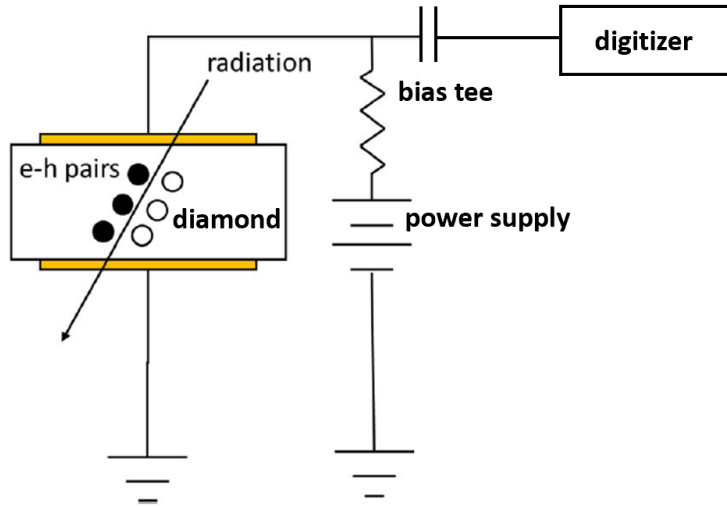


Figure 4-2: Circuit diagram of diamond diode on DARHT Axis 1

Figure 4-2 shows the schematic of the DRD circuit on Axis 1. A simple Chemical Vapor Deposition (CVD) DRD measures the intense, short pulse of a 19.6 MeV Bremsstrahlung radiation source, with dosages of  $\approx 8000$  R at 60-ns.

## Diamond Radiation Detector (DRD)

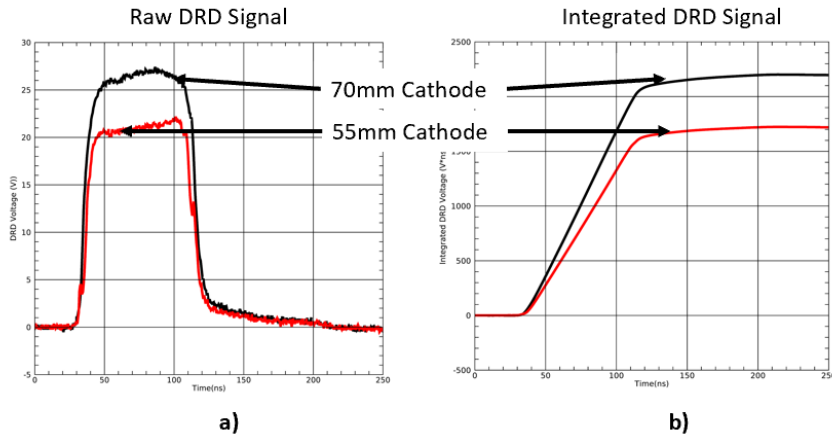


Figure 4-3: Digitized waveforms from the Diamond Radiation Detector (DRD) for both 55mm (Shot number: 39253) and 70mm (Shot number: 39290) cathodes — a) is raw waveform with 50V bias, and b) is the integrated waveform

The bias voltage across the diamond crystal was set to 50V and the DRD was calibrated at a single dose of 600 R at 1m distance. However, it does not scale properly when the dose is increased or decreased. Figure 4-3a shows the raw waveforms from the DRD and 4-2b is the numerical integration of 4-2a. The ratio of 70mm to 55mm for the integrated values averaged over 200ns of the flat top of the signal is:

$$\frac{D_{70mm}}{D_{55mm}} = 1.278 \pm 0.013 \quad (3)$$

where the expected ratio is between 1.5 and 1.6. In a conversation with [4] via email, he stated that the bias should be 1V per micron on diamond, which would imply a 1kV bias compared to our 50V bias. He had also suggested that we vary the dose and plot an I-V curve for the bias at each dose and look for linearity. If the curve is non-linear, that suggests there are insufficient charge carriers and that the voltage needs to be raised. In comparing Axis 1 and 2 DRD results, the dose rate is the only difference. The dose rate on Axis 2 is constant as the dose is increased and the the scaling is correct for low to high doses. For Axis 1 the dose rate increases by a factor of 1.53 between the 70 and 55mm cathodes. This may be why there is disagreement in the scaling of high and low doses for Axis 1. Increasing the bias voltage as stated above may resolve this issue.

## 5 Compton Diode (CD)

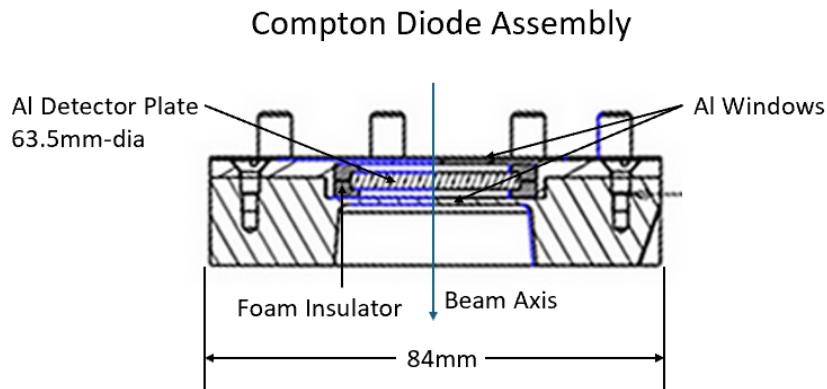


Figure 5-1: Drawing of a slice through the center of the Compton diode

Another method for measuring dose absorption is by using a Compton diode. Figure 5-1 is a drawing of the Compton diode which is then mounted on the beam axis within the safety vessel. The Bremsstrahlung radiation striking the Compton diode is collimated by the shielding aperture to an opening half-angle relative to the beam axis of  $4.28^\circ$ . This produces a radiation diameter of 19.98 mm, which is well inside of the 35 mm-diameter aluminum detector plate. The radiation distribution on the detector plate is not uniform and calculations indicate it varies center to edge by as much as 27%. The shape of the 70mm and 55mm distribution are exactly the same to less than 0.1%.

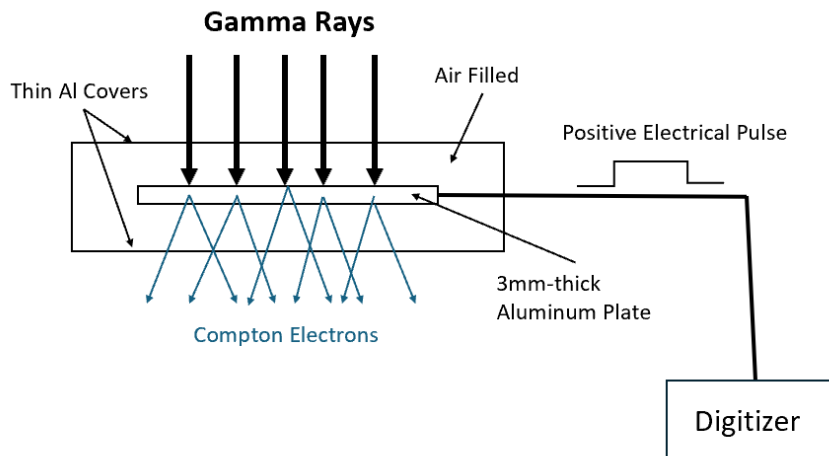


Figure 5-2: Circuit diagram of Compton diode on DARHT Axis 1

Figure 5-2 is a circuit diagram of how the Compton diode works. The radiation, in the form of Bremsstrahlung, strikes the detector plate that is connected to the center conductor of a coaxial cable, then electrons are removed from the plate by Compton scattering and a positive electrical pulse is sent to a digitizing scope to produce a time-resolved waveform. Figure 5-3 shows these

## Compton Diode (CD)

time-resolved waveforms for the 70 and 55mm cathodes, both in raw form (5-3a) and integrated 5-3b. We can see that the shapes of the raw waveforms differ dramatically, where this difference in waveform shape cannot be explained. Lastly, the ratio of the integrated values of the 70mm and 55mm averaged from 400 to 500ns is given by:

$$\frac{D_{70mm}}{D_{55mm}} = 1.695 \pm 0.002 \quad (4)$$

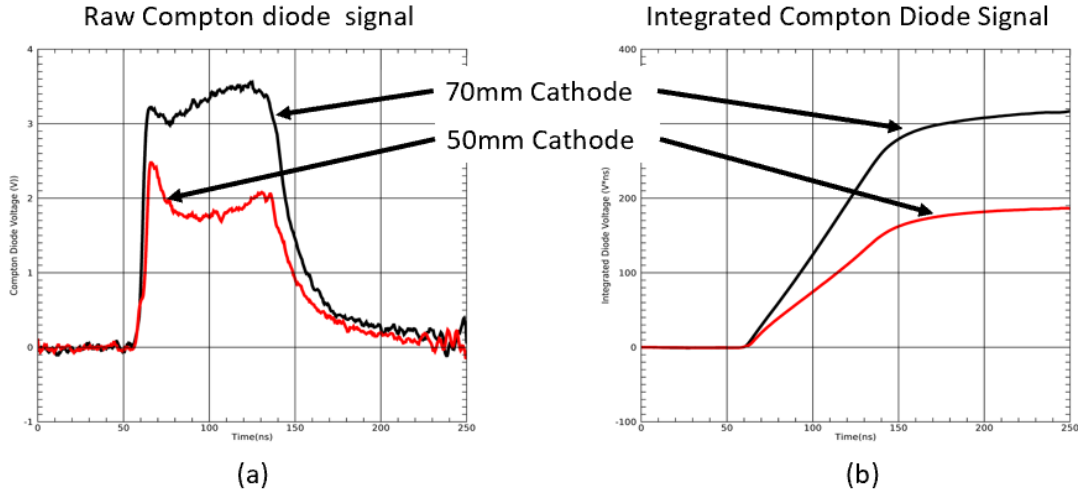


Figure 5-3: Digitized waveforms from the Compton diode for both 55mm (Shot number: 39253) and 70mm (Shot number: 39290) cathodes — a) is raw waveform, and b) is integrated waveform

## 6 Simple Scaling and xtr with Dosecalx Calculations

### 6.1 Scaling

Cathode Size	Energy (MeV)	BPM25 Charge (C)	BPM26 Charge (C)	25/26 Number of Electrons
55mm	19.60 $\pm$ 0.02	0.111 $\pm$ 0.001	0.104 $\pm$ 0.001	6.9/6.5e14
70mm	19.30 $\pm$ 0.01	0.170 $\pm$ 0.001	0.163 $\pm$ 0.002	1.06/1.02e15

Table 6-1: Summary of the accelerator parameters for the 55mm and 70mm cathodes

Calculation of the dose measurement requires the charge and beam kinetic energy on the tantalum target. Table 6-1 above is a summary of these parameters for the experiment. The beam energy is extracted from the sum of the electron spectrometer, calibrated injector, and cell electronic diagnostics (See references [3], [5], and [7]), and the the total charge is calculated by integrating the beam current waveform. Scaling of the dose follows the equation:

$$D = kQT^{2.8} \quad (5)$$

where  $D$  is dose,  $k$  is a constant scaling factor,  $Q$  is the electron charge, and  $T$  is the laboratory kinetic energy of the electrons. Assuming that  $k$  is the same for both cathodes, a reasonable assumption that which we will discuss more later, the ratio of the two doses is:

$$\frac{D_{70mm}}{D_{55mm}} = (Q_{70mm}/Q_{55mm})(T_{70mm}/T_{55mm})^{2.8} \quad (6)$$

Using the values from table 6-1 for the Charge of BPM25 gives us:

$$\frac{D_{70mm}}{D_{55mm}} = 1.467 \quad (7)$$

and using the values for the Charge of BPM26 gives:

$$\frac{D_{70mm}}{D_{55mm}} = 1.501 \quad (8)$$

indicating that slightly more charge (2.3%) is lost between BPM25 and BPM26 for the 55mm cathode.

## Simple Scaling and xtr with Dosecalcx Calculations

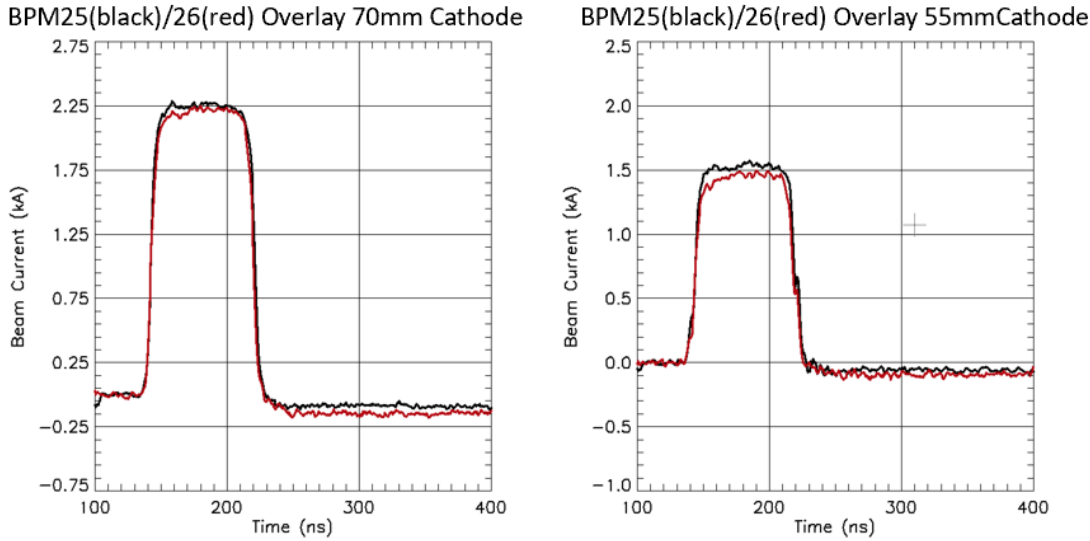


Figure 6-1: Digitized waveforms from the BPM 25 (black) and 26 (red) for both a 70mm cathode (Shot number: 39290) and a 55mm cathode (Shot number: 39256)

The difference in charge between the two BPMs can be seen when displaying the waveforms for the beam current at BPM25 and BPM26 for both the 70mm and 55mm cathodes, shown in Figure 6-1. BPM 25 is a standard calibrated current/position monitor, while BPM26 is a non-standard monitor that has not been calibrated and relies only on a scaled estimate.

### 6.2 Dosecalcx and xtr

Dosecalcx [2] is a useful program used for thick target Bremsstrahlung, where it that calculates on-axis dose and photon distributions over small half-angles less than  $6^\circ$ . The inputs to Dosecalcx can be seen in table 6-2:

Dosecalcx Input	55mm Cathode	70mm Cathode
Electron Energy (MeV)	19.60	19.30
Convergence Angle (Degrees)	5.16	4.98
Max Gamma angle (Degrees)	4.28	4.28
Number of electrons (BPM26)	6.05e14	1.02e15
Target Material	Ta	Ta
Target Thickness ( $g/cm^2$ )	1.669	1.669
Filter Material	Al	Al
Filter Thickness ( $g/cm^2$ )	0.27	0.27
On Axis Dose @ 1m	417	671

Table 6-2: Summary of the Dosecalcx input parameters for the 55mm and 70mm cathodes

## Simple Scaling and xtr with Dosecalcx Calculations

Using the beam envelope code xtr, we are able to calculate the beam convergence angle for both the 55mm and 70mm cathodes. The beam envelopes were shown earlier in Figure 2-2, and the resulting phase-space plots are shown in figure 6-2.

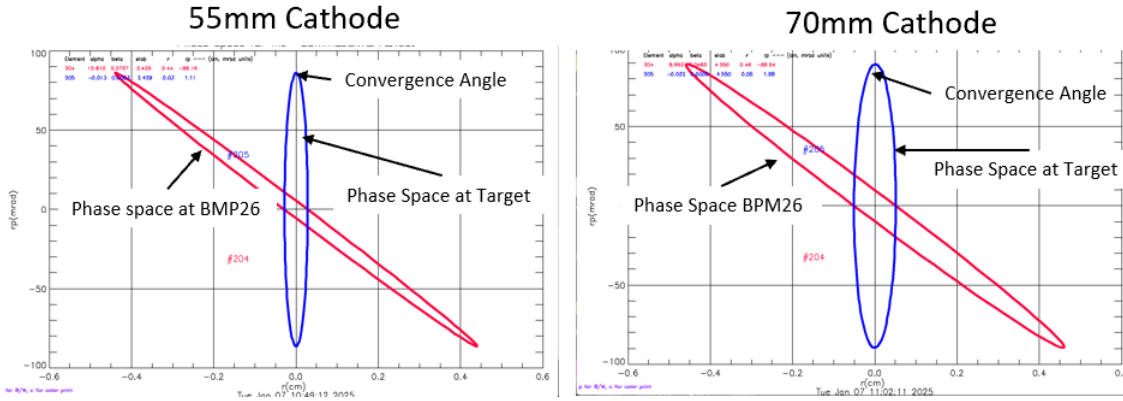


Figure 6-2: Twiss plots calculated by xtr for transport from BPM26 to the target for 55mm and 70mm cathode using respective xtr tunes.

Both cathodes have similar convergence angles as seen in the plots, with the exact values being  $5.16^\circ$  for the 55mm cathode, and  $4.98^\circ$  for the 70mm cathode. The remaining inputs in table 6-2 are taken from the analysis of with material characteristics and waveforms of shot data from figure 6-1.

The dose scaling factor for Dosecalcx is calculated by the ratio of the two doses for each cathode, which gives us:

$$\frac{D_{70mm}}{D_{55mm}} = 1.61 \quad (9)$$

and the above scaling factor can be used to compare the signal shapes and amplitudes from the DRD and Compton diode, as shown in Figure 6-3.

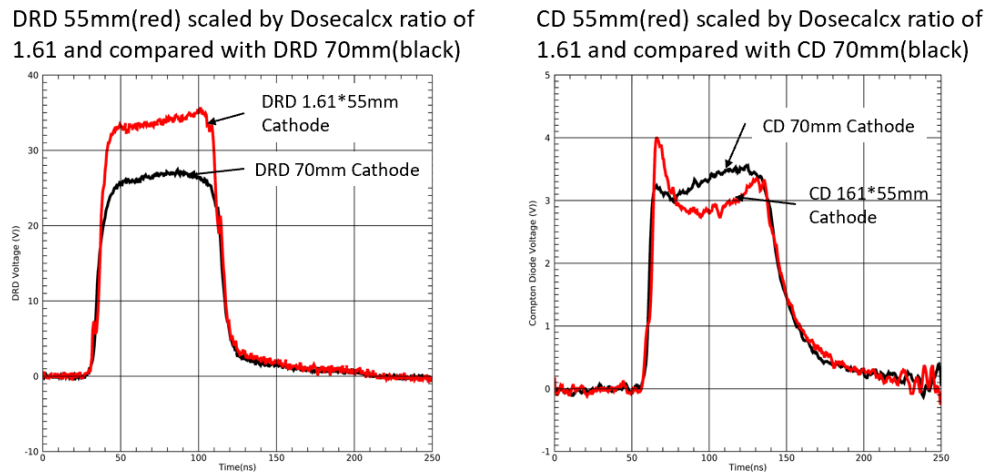


Figure 6-3: DRD (a) and CD (b) for 55mm (Red) and 70mm (black) with Dosecalcx scaled values for 55mm waveforms.

## **Simple Scaling and xtr with Dosecalcx Calculations**

The plots show us that the DRD waveforms in fact do not match, and this problem likely arises from the 50V bias voltage amplitude on the diamond. It is much too small compared to an ideal bias voltage of 1kV, and as a consequence, insufficient electron-hole pairs are produced. Unfortunately, this ideal 1kV voltage is not achievable in our geometry. Furthermore, The CD waveforms are comparable when scaled, and the structure of the details is of interest. There are two possible explanations for this difference: it could either stem from electronic response of the CD system or result from effects within the target. Current efforts are directed toward eliminating the electronic response of the system.

## 7 Conclusion

In this paper, we explored several techniques for determining the x-ray dose for two different beam currents produced by a 55mm and 70mm diameter cathode, including calorimetry, the use of a Diamond Radiation Detector, and using a Compton Diode. However, our data suggests that obtaining an accurate measurement of dose is elusive. The dose does not scale consistently with cathode size and the on-axis dose is different, both with and without the collimator, and the ratios of the the 70mm/55mm cathodes all widely vary with relatively small statistical errors (see Table 7-1).

Calorimeter	Diamond Radiation Detector	Compton Diode	Simple Scaling	Dosecalcx
$1.84 \pm 0.02$	$1.278 \pm 0.013$	$1.695 \pm 0.002$	$1.484 \pm 0.017$	$1.61 \pm 0.02$

Table 7-1: Ratios of radiation measurements for 55mm and 70mm cathodes

The bias voltage on the Diamond Radiation Detector is much too low at 50V when compared to an ideal voltage of 1kV. The difference in dose rates between the 55mm and 70mm cathodes may be responsible for the apparent saturation of the 70mm DRD signal at the same bias voltage as the 55mm data shown in Figure 6-3. In the same figure, the two CD signals for the 70mm and 55mm have roughly the same scaled amplitude, but the shapes are vastly different. The Compton diode for the 55mm cathode has a shape that would indicate the impedance is inductive, which can be seen by in the waveform overshooting at the front of the signal and gradually decaying at the end. The 70mm cathode waveform, on the other hand, is much different. There is a small inductive overshoot and a rising amplitude in the main body, and it is as if the electrical circuit is changing with intensity or the radiation temporal distribution changes with target interaction.

In future experiments, several issues with the experimental set-up will be addressed. First and foremost is the alignment of the assembly. The next experiment will have on-axis laser, allowing for precise and accurate alignment. Secondly, a more complete set of Gafchromic film measurements need to be made of radiation distributions, and the bias voltage of the DRD will be varied for each intensity in order to determine an optimum setting. Lastly, the electrical response of the Compton diode needs to be characterized and optimized, which will enable physics interpretation of the output signal. When put in use, all of these changes will allow for more accurate and precise x-ray dose measurements on Axis 1 and the DARHT Facility.

## References

- [1] P. W. Allison. *xtr a New Beam Dynamics Code*. Tech. rep. DARHT Technical Note No. 50. Los Alamos National Laboratory (LANL), Jan. 1995.
- [2] B. T. Largent T. J. Burris-Mog and D. C. Moir. *DOSECALCX, A Bremsstrahlung Radiation Dose Code for Electron Beam Targets*. Tech. rep. LA-UR-18-31394. Los Alamos National Laboratory (LANL), Dec. 2018.
- [3] D. C. Moir T. Burris-Mog and B. T. McCuistian. *Linear Induction Accelerator Cell Voltage Calibration Using Compact Electron Permanent Magnet Spectrometer*. Tech. rep. LA-UR-19-30140. Los Alamos National Laboratory (LANL), Oct. 2019.
- [4] Jason Holmes. “Private communication”. email.
- [5] D. C. Moir T. Burris-Mog N. Kallas M J Jaworski and B T McCuistian. *Optimization of DARHT Axis 1 Injector Voltage*. Tech. rep. LA-UR-20-23236. Los Alamos National Laboratory (LANL), Aug. 2020.
- [6] S. A. Watson T. Kauppila and K. H. Mueller. *A Cryogenic Dose Calorimeter for Pulsed Radiographic Facilities*. Tech. rep. DARHT Technical Note No. 47. Los Alamos National Laboratory (LANL), Oct. 1994.
- [7] M. J. Jaworski N. Kallas B. T. McCuistian and D. C. Moir. *Transfer Function Identification and Cross-Calibration of E-dot Sensors via Bayesian Inference in a Linear Induction Accelerator*. Tech. rep. LA-UR-23-26812. Los Alamos National Laboratory (LANL), June 2023.